



# Microbiome-Derived Lipopolysaccharide (LPS) Selectively Inhibits Neurofilament Light Chain (NF-L) Gene Expression in Human Neuronal-Glial (HNG) Cells in Primary Culture

Walter J. Lukiw<sup>1,2,3\*</sup>, Lin Cong<sup>4</sup>, Vivian Jaber<sup>1</sup> and Yuhai Zhao<sup>1,5</sup>

<sup>1</sup> Neuroscience Center, Louisiana State University School of Medicine, Louisiana State University Health Sciences Center, New Orleans, LA, United States, <sup>2</sup> Department of Neurology, Louisiana State University School of Medicine, Louisiana State University Health Sciences Center, New Orleans, LA, United States, <sup>3</sup> Department of Ophthalmology, Louisiana State University School of Medicine, Louisiana State University Health Sciences Center, New Orleans, LA, United States, <sup>4</sup> Department of Neurology, Shengjing Hospital, China Medical University, Shenyang, China, <sup>5</sup> Department of Anatomy and Cell Biology, Louisiana State University School of Medicine, Louisiana State University Health Sciences Center, New Orleans, LA, United States

## OPEN ACCESS

### Edited by:

Ioannis Dragatsis,  
University of Tennessee Health  
Science Center (UTHSC),  
United States

### Reviewed by:

Fernanda Marques,  
Instituto de Pesquisa em Ciências da  
Vida e da Saúde (ICVS), Portugal  
Cheryl Wellington,  
University of British Columbia,  
Canada

### \*Correspondence:

Walter J. Lukiw  
wlukiw@lsuhsc.edu

### Specialty section:

This article was submitted to  
Neurogenomics,  
a section of the journal  
Frontiers in Neuroscience

**Received:** 07 March 2018

**Accepted:** 16 November 2018

**Published:** 05 December 2018

### Citation:

Lukiw WJ, Cong L, Jaber V and  
Zhao Y (2018) Microbiome-Derived  
Lipopolysaccharide (LPS) Selectively  
Inhibits Neurofilament Light Chain  
(NF-L) Gene Expression in Human  
Neuronal-Glial (HNG) Cells in Primary  
Culture. *Front. Neurosci.* 12:896.  
doi: 10.3389/fnins.2018.00896

The remarkable co-localization of highly pro-inflammatory lipopolysaccharide (LPS) with sporadic Alzheimer's disease (AD)-affected neuronal nuclei suggests that there may be some novel pathogenic contribution of this heat stable neurotoxin to neuronal activity and neuron-specific gene expression. In this communication we show for the first time: (i) the association and envelopment of sporadic AD neuronal nuclei with LPS in multiple AD neocortical tissue samples; and (ii) a selective repression in the output of neuron-specific neurofilament light (NF-L) chain messenger RNA (mRNA), perhaps as a consequence of this association. The down-regulation of NF-L mRNA and protein is a characteristic attribute of AD brain and accompanies neuronal atrophy and an associated loss of neuronal architecture with synaptic deficits. To study this phenomenon further, human neuronal-glial (HNG) cells in primary culture were incubated with LPS, and DNA arrays, Northern, Western, and ELISA analyses were used to quantify transcription patterns for the three member neuron-specific intermediate filament-gene family NF-H, NF-M, and NF-L. As in sporadic AD limbic-regions, down-regulated transcription products for the NF-L intermediate filament protein was significant. These results support our novel hypothesis: (i) that internally sourced, microbiome-derived neurotoxins such as LPS contribute to a progressive disruption in the read-out of neuron-specific genetic-information; (ii) that the presence of LPS-enveloped neuronal nuclei is associated with a down-regulation in NF-L expression, a key neuron-specific cytoskeletal component; and (iii) this may have a bearing on progressive neuronal atrophy, loss of synaptic-contact and disruption of neuronal architecture, all of which are characteristic pathological

features of sporadic-AD brain. This is the first report that provides evidence for a neuron-specific effect of a human GI-tract microbiome-derived neurotoxin on decreased NF-L abundance in both sporadic AD temporal lobe neocortex *in vivo* and in LPS-stressed HNG cells *in vitro*.

**Keywords:** Alzheimer's disease (AD), DNA array, inflammatory degeneration, lipopolysaccharide (LPS), microbiome, neurofilament light chain (NF-L), neurofilament triplet

## INTRODUCTION

Recently there has been a resurgence of interest in the human gastrointestinal (GI) tract microbiome and its potential contribution to human health and disease. One area receiving considerable research attention has been the possible involvement of human GI-tract microbiome-derived neurotoxins with progressive and terminal neurological diseases associated with aging and inflammatory neurodegeneration. These microbiome-derived neurotoxic exudates consist of a remarkably complex and neurobiologically potent array of pro-inflammatory endotoxins and exotoxins (such as flagellin), lipooligosaccharides (LOS), lipopolysaccharides (LPS; including the extremely pro-inflammatory *B. fragilis* LPS, BF-LPS), microRNA-like small non-coding RNAs (sncRNA), and an extensive variety of bacterial-derived amyloids (Hofer, 2014; Foster et al., 2016; Lukiw, 2016a,b; Zhan et al., 2016, 2018; Mancuso and Santangelo, 2017; Yang and Chiu, 2017; Zhao et al., 2017a,b,c; Zhao and Lukiw, 2018). Several recent papers have addressed the emerging link between elements of the human GI-tract microbiome and Alzheimer's disease (AD), a common, chronic, and progressive age-related neurodegenerative disease whose incidence is reaching epidemic proportions and represents a major, lethal, neuropsychiatric disorder that currently constitutes a major healthcare concern worldwide (Zhan et al., 2016; Jiang et al., 2017; Cox and Weiner, 2018; Szablewski, 2018; Zhao and Lukiw, 2018).

Both the familial and the much more common sporadic forms of AD are characterized by the appearance of extracellular deposits including dense, insoluble amyloid-beta (A $\beta$ ) peptide enriched senile plaques (SP) and tau- and neurofilament-protein enriched neurofibrillary tangles (NFT), and neuropathologically by the progressive atrophy of large neurons, ensuing loss of synaptic contacts and altered neuronal cytoarchitecture (Clark and Vissel, 2015; Zhao and Lukiw, 2015; Minter et al., 2016). We adopted the strategy that because inter-synaptic connections, the radial diameter of neurons and the overall neuronal architecture and morphology are maintained in large part by this relatively abundant three member neuron-specific neurofilament gene family – encoding the neurofilament light (NF-L; NEFL; 68 kDa), neurofilament medium (NF-M; ~160 kDa), and neurofilament heavy (NF-H; ~205 kDa) chain proteins – we reasoned that NF-L, NF-M, and NF-H relative abundance would be an experimentally practical and suitable choice to look for changes in expression in both sporadic AD brain and in LPS treated human neuronal-glia (HNG) cells in primary culture.

Our findings indicate for the first time, that linked to a progressive association of the amphiphilic glycolipid LPS with

sporadic AD neuronal nuclei there appears to be a parallel and selective repression in the output of neuron-specific NF-L mRNA in AD brain compared to age- and gender-matched controls. This is noteworthy because down-regulation of NF-L expression is a characteristic feature of the limbic system in AD and accompanies the atrophy of neurons and progressive loss of neuronal architecture and synaptic contact in the AD brain (McLachlan et al., 1988; Lukiw et al., 1990; Julien and Mushynski, 1998; Clement et al., 2016; Khalil et al., 2018). These effects were further observed in HNG primary cultures incubated with Gram-negative bacterial-derived LPS in which was observed a significant LPS-mediated down-regulation of the NF-L intermediate filament protein. Taken together these results suggest: (i) that microbiome-derived LPS may contribute to a progressive disruption in the read-out of the brain's neuron-specific genetic information; (ii) that NF-L mRNA and the expression of NF-L proteins are one important neuron-specific transcript targeted by microbiome-derived LPS; and (iii) that this may have a bearing on neuronal atrophy, disruption of the neuronal architecture and loss of synaptic organization, all of which are characteristic neuropathological features of AD-affected brain.

## MATERIALS AND METHODS

### Human Brain Tissues, Antibodies and Immunohistochemistry

Female control [ $N = 12$ ; mean age  $\pm$  one standard deviation of  $85.8 \pm 2.1$  years with a post-mortem interval (PMI) of (mean  $\pm$  one standard deviation)  $3.6 \pm 1.5$  h] and age-matched AD ( $N = 12$ ; age  $87.7 \pm 2.5$  years and PMI  $3.8 \pm 1.2$  h) human superior temporal lobe neocortical tissues (Brodmann A22) were obtained from the University of Maryland, from archived material at the University of Toronto and the Louisiana State University Neuroscience Center, and the University of California (UC)-Irvine Brain Bank. A total of 24 female, age-, gender-, and PMI-matched control and AD brains were examined for LPS content. For immunocytochemistry of LPS human brain tissue samples were embedded in OCT and frozen at  $-80^{\circ}\text{C}$ ;  $10 \mu\text{m}$  brain sections were cut using a Shandon cryotome (Waltham, MA, United States). After an initial fixation with 4% paraformaldehyde for 20 min, sections were then incubated in primary antibodies (1:1000;  $1 \times$  PBS with 2% BSA, 2% goat or donkey serum and 0.1% TX-100) overnight at  $4^{\circ}\text{C}$ , washed with PBS, and then incubated with Alexa Fluor-conjugated species-specific secondary antibodies (ThermoFisher Scientific,

Waltham, MA, United States) for 3 h at RT (see further details below). Sections were counter-stained with DAPI for nuclei, followed by quenching with Autofluorescence Eliminator Reagent (Millipore Cat No. 2160; Zhan et al., 2016; Zhao et al., 2017a,b,c), mounted on glass slides, cover-slipped with Fluoromount-G (ThermoFisher Scientific) and imaged using a Zeiss LSM 700 Confocal Laser Scanning microscope system (Carl Zeiss Microscopy, Thornwood, NY, United States; Bagyinszky et al., 2017; Zhao et al., 2017a,b,c<sup>1</sup>).

### Human Neuronal-Glial (HNG) Cells in Primary Co-culture

Human neuronal-glia primary cells, cryopreserved at first passage one, were obtained from commercial sources and cultured according to the manufacturer's instructions (Lonza PT-2599, Lonza Cell Systems, Allendale, NJ, United States or Cell Systems, ACBRI 376, Kirkland, WA, United States). HNG cells tested negative for HIV-1, HBV, HCV, mycoplasma, bacteria, yeast, and fungi at source, and have been extensively used for studies on brain gene induction and gene expression, neuronal development, neurotoxicology, neuropharmacology, and in *in vitro* models of AD and other age-related neurological disorders that exhibit a progressive age-related inflammatory neurodegeneration (Li et al., 2011; Zhao et al., 2017a,b,c; Zhao and Lukiw, 2018). HNG cells demonstrate particular neuronal and astroglial cell markers including neuron-specific  $\beta$ -tubulin III ( $\beta$ tubIII; red staining;  $\lambda_{\text{max}} = 690$  nm) and glial fibrillary acidic protein (GFAP; glial-specific green stain;  $\lambda_{\text{max}} = 520$  nm). Briefly, HNG cells were maintained as free-floating aggregates (neurospheres) in 75 cm<sup>2</sup> uncoated plastic flask in neural progenitor maintenance media (NPM; Lonza CC-3209) supplemented with recombinant human fibroblast

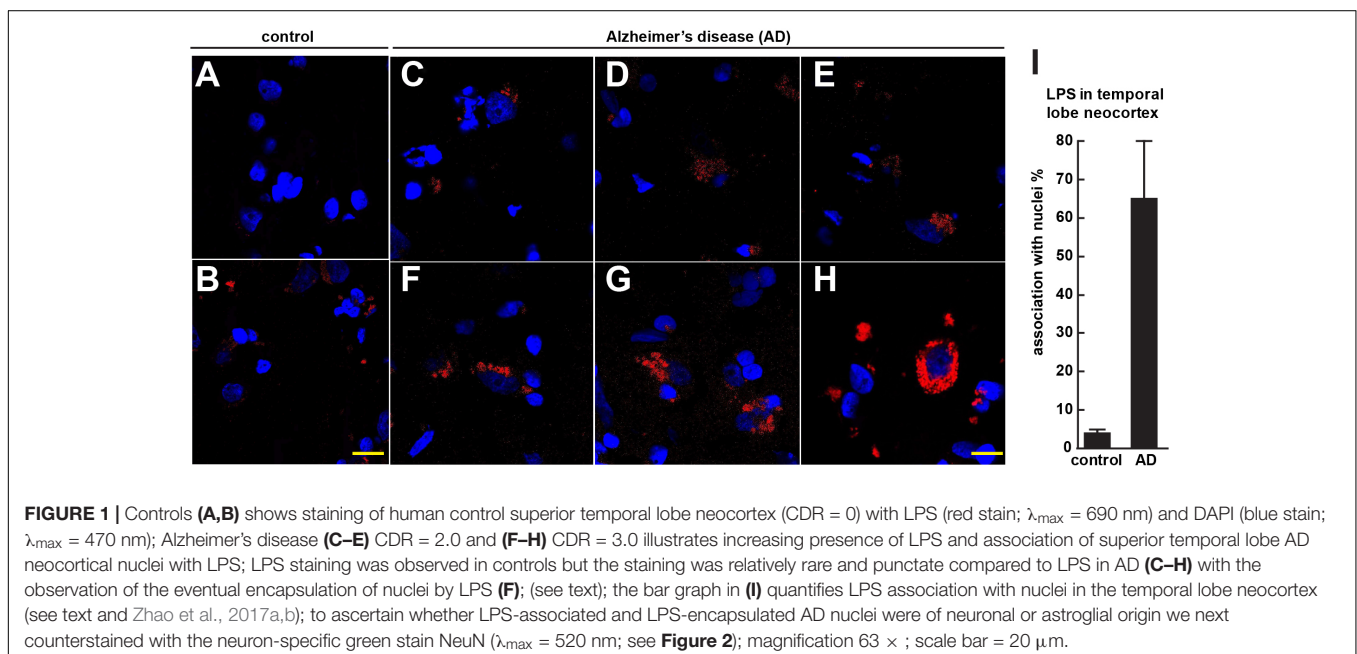
growth factor (rhFGF) and epidermal growth factor [rhEGF] and neural survival factor-1 [NSF-1] (Lonza CC-4242) and gentamicin/amphotericin-B (Lonza GA-1000). Differentiation was induced by plating neurospheres onto eight-well glass chamber-slides pre-coated with poly-L-ornithine (an amino acid polymer used as substratum to improve neuronal adhesion); cells were kept at 37°C in a humidified 5% CO<sub>2</sub> atmosphere incubator at all times. The differentiation media (Lonza CC-4242) was free of growth factors but contained NSF and gentamicin/amphotericin-B, 25 ng/ml of brain-derived neurotrophic factor (BDNF), and 1% of fetal bovine serum (FBS). Upon deprivation of growth factors neurospheres began to attach to the well bottoms and next migrated out to form a co-culture of human neurons and glial cells (HNG). HNG cells were used 2 weeks after induction of differentiation; HNG cells initially contained about  $5 \times 10^5$  cells/ml volume and were cultured to ~70% confluency in HNG cell medium as described in detail (Cui et al., 2010; Bhattacharjee and Lukiw, 2013; Zhao et al., 2014, 2017a,b,c; Lukiw, 2016a,b). HNG cells were subsequently incubated with LPS; the concentration of LPS (Sigma L2630<sup>2</sup>) provided to 2-week-old HNG cells cultured in HNG cell medium was 50 nM for 48 h (see **Figure 4**; for further specific details see also Zhao et al., 2017a,b,c). Higher doses of LPS (up to 5  $\mu$ M) in HNG cell medium for shorter periods gave comparable results (data not shown).

### Immunofluorescence Protocol

Two week old cultures of HNG cells in eight-well chamber slides (BD Biosciences, San Jose, CA, United States) were fixed with 4% paraformaldehyde, then permeabilized and blocked with 0.125% Triton X-100 and 2% normal goat serum in PBS at RT for 1 h. Cells were incubated overnight at 4°C

<sup>1</sup>[https://www.mikroskop.com.pl/pdf/LSM700\\_1.pdf](https://www.mikroskop.com.pl/pdf/LSM700_1.pdf)

<sup>2</sup><https://www.sigmaaldrich.com>



with antibodies for  $\beta$ -tubulin III (for neurons; Sigma T8578, Sigma-Aldrich St. Louis, MO, United States) and GFAP (for astrocytes; Sigma G9629). Cells were subsequently washed for three times with PBS and then incubated for 3 h at room temperature with secondary antibodies conjugated with cy3 or FITC fluorescein (ThermoFisher A21422 and A11008; ThermoFisher Scientific, Waltham, MA, United States). After washing and drying, slides were applied with mounting medium containing DAPI (1:10,000; Vector Laboratories, Burlingame, CA, United States) and observed under Zeiss Axioplan Inverted Deconvolution Fluorescent Microscope (63 $\times$  oil immersion lens; Carl Zeiss, Oberkochen, Germany). Positively stained cells were quantified manually using the manual counter function of ImageJ software (NIH). Negative control with quenching was performed as previously reported in detail (Zhao et al., 2017a,b,c); quantification of LPS was analyzed (i) as a percentage of neuronal area (see below); and/or (ii) by counting multiple microscope fields for the quantity of LPS signals (red stain;  $\lambda_{\text{max}} = 690$  nm) associated with DAPI (blue nuclear stain;  $\lambda_{\text{max}} = 470$  nm) (see **Figures 1–3**).

### Antibodies – Specificity and Validation

We used mouse anti-*E. coli* LPS (Abcam Cat No. ab35654; Cambridge, MA, United States); rabbit anti-NeuN (Cell Signaling, Cat No. 24307), rabbit anti-GFAP (Sigma-Aldrich, Cat No. G4564) (Cui et al., 2010; Zhao et al., 2014; Lukiw, 2016a, 2017; Zhan et al., 2016). LPS antibody specificity and validation was confirmed (i) using Western immunoblot analysis (see **Figure 1** in Zhao et al., 2017a) which corresponded to the manufacturer's published specifications<sup>3</sup>; and (ii) an antibody neutralization/LPS quenching control assay (Zhao et al., 2017a,b,c). We used sandwich ELISA and Western analysis for NF-L protein determination in LPS-treated HNG cells using Abxexa (abx250460; Cambridge, United Kingdom) and/or LifeSpan BioSciences (LSBio; LS-F6701; Seattle, WA, United States) ELISA systems and NF-L (NEFL) monoclonal antibody (DA2; ThermoFisher Scientific, Cat No. MA1-2010) and a beta actin ( $\beta$ -actin) loading control monoclonal antibody (BA3R; ThermoFisher Scientific, Cat No. MA5-15739) and standard Western analysis as has been previously described by our laboratory (Zhao et al., 2017a,c). To ascertain the association of LPS with neuronal cells confocal images of LPS and NeuN staining were imported into ImageJ<sup>4</sup>; RGB images were first converted into images of separate channels (red for LPS; green for NeuN; and blue for DAPI-stained nuclei). A co-localization finder plugin was run to generate images of co-localization of both channels; each co-localization image was converted into an 8-bit image and inverted. Global thresholding was utilized and the cutoff value was adjusted to the point that only highlighted co-localized particles are black on the image against a white background. Particle analysis was next performed to calculate the area size of the co-localization; this value was then divided by the area size

of the NeuN or DAPI staining as the percentage of cell area (Zhao et al., 2017a,b).

### RNA Isolation and Purification, DNA Array, Northern, ELISA, and Western Analysis

Ultrapure chemicals and reagents of the highest grades commercially available were used throughout these experiments. Typically, 10 mM phenylmethylsulfonyl fluoride (PMSF; Sigma) and 1 U human placenta ribonuclease inhibitor (RNasin; Promega Corporation, Madison WI, United States) were employed in the extraction medium to inhibit protease and specific ribonuclease activities in homogenized human brain tissues or HNG cells. Total cellular RNA was isolated using TRIzol Reagent (Invitrogen-ThermoFisher Scientific; Cat No. 15596026) and quality controlled using analysis using and Agilent 2100 bioanalyzer (Agilent Technologies, Santa Clara CA, United States). For Northern blots  $\sim 15$   $\mu$ g of total RNA was separated at 4°C on 1.5% agarose/2.2 M formaldehyde gels at 60 V for 15 h with recirculating 20 mM sodium phosphate buffer, pH 7.0. Gels were stained for 10 min with acridine orange, visualized at 340 nm on a UV trans-illuminator and total RNA was blotted onto Biotrans 0.2  $\mu$ m Biotrans nylon membrane (Cat No. 01811300, MP Biomedicals). NF-H, NF-M, and NF-L probes were prepared to specific activities of  $10^8$  dpm <sup>32</sup>p-labeled dCTP per/ $\mu$ g of DNA as previously described in detail (Clement et al., 2016). Membranes were pre-hybridized for 12 h at 42°C in 50% formamide, 5 $\times$  Denhardt's solution (containing 0.1% each of Ficoll 400, polyvinylpyrrolidone, and bovine serum albumin), 5 $\times$  SSC (standard saline citrate, containing 150 mM sodium chloride, 15 mM sodium citrate, pH 7.0), 50 mM sodium phosphate buffer, pH 6.5, 0.1% sodium dodecyl sulfate (SDS), and 350  $\mu$ g/ml sonicated herring sperm. This was replaced with fresh hybridization solution containing approximately  $5 \times 10^7$  cpm of heat-denatured cDNA probes and hybridization occurred at 42°C for 30 h. Nylon membranes were washed under conditions of high stringency (two 30-min washes at 2  $\times$  SSC/0.1% SDS at room temperature; two 60-min washes at 0.1 $\times$  SSC/0.5% SDS at 60–65°C and finally two 15-min washes at 1  $\times$  SSC/0.1% SDS at room temperature). When used Fuji RX film was exposed at  $-70^\circ\text{C}$  for 18–72 h using standard autoradiographic imaging techniques; alternately hybridization signals were quantified using a Typhoon FLA 9500 Biomolecular Imager (GE Healthcare). DNA array analysis was performed as extensively described by our group (Colangelo et al., 2002; Clement et al., 2016; Jaber et al., 2017). Sandwich ELISA and/or Western analysis was used for NF-L protein abundance analysis according to the manufacturers' instructions to quantify both NF-L and  $\beta$ -actin control abundance levels (**Figure 4**).

### Statistical Analysis, Integrated Bioinformatics Analysis, and Data Interpretation

For NF-H, NF-M, NF-L,  $\beta$ -actin, and GAPDH mRNA abundance analysis all statistical procedures were analyzed using *p*, analysis of variance (ANOVA) a two-way factorial analysis of variance

<sup>3</sup><http://www.abcam.com/e-coli-lps-antibody-ab211144.html>

<sup>4</sup><https://imagej.net/Fiji/Downloads>

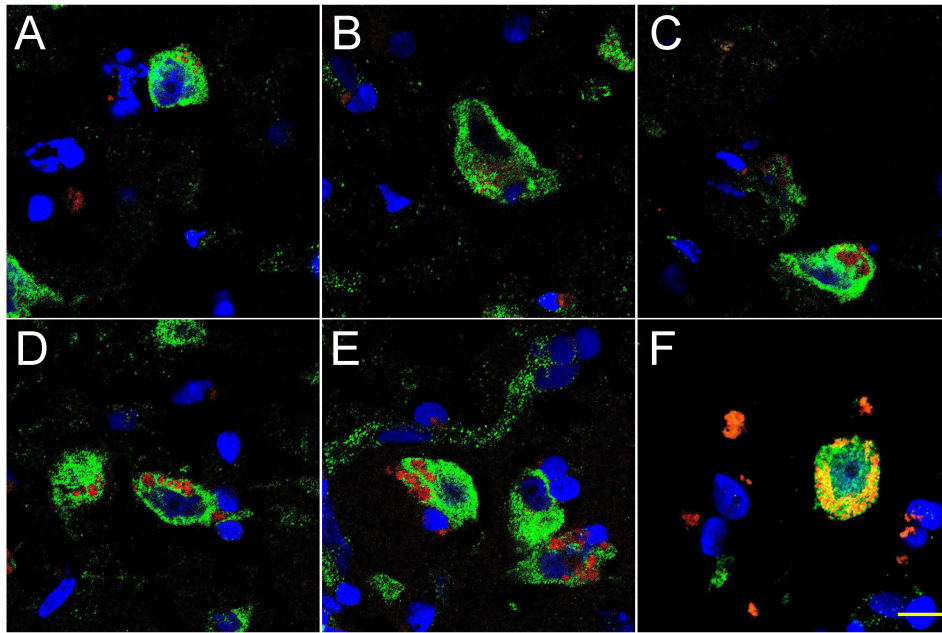


**FIGURE 2 |** Progressive association and envelopment of AD-affected neocortical neuronal nuclei by LPS (red stain;  $\lambda_{\text{max}} = 690$  nm), DAPI (blue nuclear stain;  $\lambda_{\text{max}} = 470$  nm) and NeuN (neuron-specific green stain;  $\lambda_{\text{max}} = 520$  nm); human superior temporal lobe AD neocortex (Brodmann A22) from CDR (clinical dementia rating) 1.0, 2.0 and 3.0 AD brains; **A,B** = CDR 1.0; **C,D** = CDR 2.0; **E,F** = CDR 3.0 (see also <https://knightadrc.wustl.edu/cdr/cdr.htm>); LPS staining (red) was subjected to co-localization analysis with the neuronal marker NeuN (green) and/or nuclear marker (blue); magnification 63 $\times$ ; scale bar = 20  $\mu\text{m}$ .

using algorithms, and/or procedures in the SAS language (Statistical Analysis Institute, Cary, NC, United States) and as previously described (Cui et al., 2010; Zhao et al., 2011; Clement et al., 2016; Dendooven and Luisi, 2017; Zhao and Lukiw, 2018). In the results *p*-values of less than 0.05 (ANOVA) were considered to be statistically significant. All NF-H, NF-M, NF-L,  $\beta$ -actin, and GAPDH mRNA abundance data were collected and analyzed using Excel 2016 (Office 365) algorithms (Microsoft Corporation, Redmond WA, United States); all figures were generated using Adobe Illustrator CC 2015 and Photoshop CC version 14.0 (Adobe Corporation, San Jose, CA, United States).

## RESULTS

**Figure 1** (control A,B) shows staining of 10  $\mu\text{m}$  brain sections of human control superior temporal lobe neocortex (Brodmann A22; CDR = 0) of **Figure 1A** an 86 year-old female, 3.6 h PMI and **Figure 1B** an 85-year-old female, 4.3 h PMI) stained with LPS (red stain;  $\lambda_{\text{max}} = 690$  nm) and DAPI (blue stain;  $\lambda_{\text{max}} = 470$  nm); control samples (A) and (B) were from patients with no history of neurodegenerative disease or cognitive impairment; LPS staining was infrequently observed in controls and the staining was sparse; Alzheimer's disease (**Figures 1C–H**); (**Figures 1C–E**) CDR = 2.0; and (**Figures 1F–H**) CDR = 3.0; all female; age-range 79–89; PMI range 3.3–4.1 h; illustrates progressive association and envelopment of AD neocortical nuclei with LPS—LPS (red stain;  $\lambda_{\text{max}} = 690$  nm) and DAPI (blue stain;  $\lambda_{\text{max}} = 470$  nm) staining of human superior temporal lobe AD neocortex (Brodmann A22);

note minor ‘punctate’ LPS signals in control (**Figures 1A,B**) not associated with nuclei, compared to LPS in AD (**Figures 1C–F**) and encapsulation of nuclei by LPS. In a previous study LPS was reported to range from a  $\sim 7$ - to  $\sim 21$ -fold increase in abundance in AD brain over age-matched controls from the same anatomical region (Zhao et al., 2017a). The bar graph in **Figure 1I** quantifies LPS association with nuclei in the temporal lobe neocortex (see text); in AD over control; this ratio is about 16.3 for the samples examined; to investigate whether LPS-encapsulated AD nuclei were of neuronal or astroglial origin we next counterstained with the neuron-specific green stain NeuN (**Figure 2**).

**Figure 2** shows 10  $\mu\text{m}$  sections of AD neocortical brain tissue stained additionally with NeuN, a neuron-specific green stain ( $\lambda_{\text{max}} = 520$  nm). Interestingly, (i) all LPS staining appears to be confined to one specific nuclear region of AD neuronal nuclei; and (ii) the entire neuronal perinuclear region was occupied by LPS stain in about 5–15% of all neuronal nuclei associated with LPS especially in the later stages of sporadic AD (CDR = 3.0).

**Figure 3** shows detail of this LPS-AD neuronal nuclear interaction; approximately 60–70% of all moderate-to-late-stage (CDR 2.0 to 3.0) AD neocortical neuronal nuclei exhibited an association with LPS and about 5–15% of all AD neuronal nuclei in the temporal lobe neocortex showed a complete envelopment by LPS in the 12 sporadic AD cases investigate in this study. Immunocytochemistry further indicated that the “thickness” of “perinuclear LPS envelopes” ranged between 2 and 20  $\mu\text{m}$  (**Figures 2, 3**).

**Figure 4** describes experiments in human neuronal-glial (HNG) cells in primary culture exposed to LPS; HNG cells

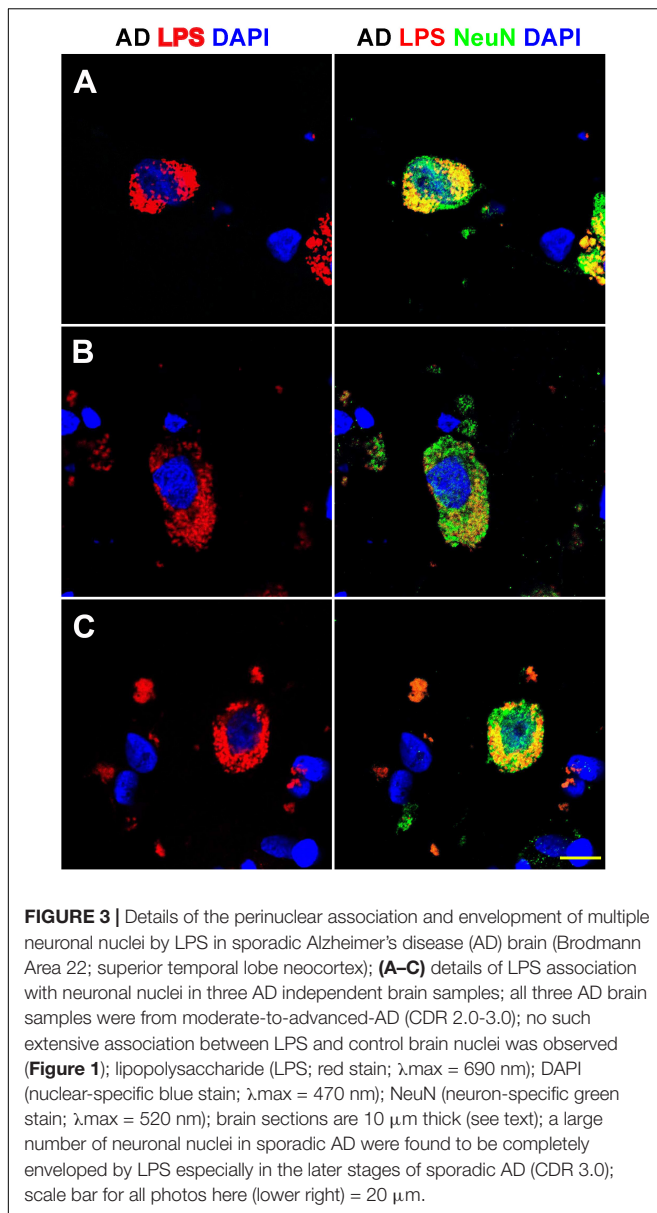


(**Figure 4A**) cultured for 2 weeks, 60% confluent and containing about 70% neurons and 30% astroglia, were exposed to 50 nM LPS for 48 h, total RNA was isolated and analyzed on DNA arrays as extensively described by our laboratories (Colangelo et al., 2002; Clement et al., 2016; Jaber et al., 2017). Even at brief periods of exposure to LPS (48 h), LPS appeared to have a strong affinity for DAPI-stained neocortical nuclei (**Figure 4B**). DNA array analysis (**Figure 4C**) indicated that in comparison to the DNA array control transcripts  $\beta$ -actin and glyceraldehyde phosphate dehydrogenase (GAPDH), NF-H mRNA, NF-M mRNA, and NF-L mRNA were found to be reduced to 0.95–0.72-, and 0.25-fold of controls; in these experiments the NF-L mRNA reduced to 0.25-fold of controls achieved the highest significance of down-regulation ( $p < 0.01$ , ANOVA); **Figure 4D** represents the quantification of these signals in bar-graph format. **Figure 4E**

shows the results of a Northern blot indicating decreased abundance of NF-L mRNA in AD versus age- and gender-matched controls and **Figure 4F** shows the quantified results in bar graph format comparing both the 4.3 and 2.6 knt NF-L mRNA abundance in control and AD. For additional details, please refer to the legend to **Figure 4**.

**Figure 5A** shows the results of a sandwich ELISA analysis confirming decreased abundance of NF-L protein in AD versus age- and gender-matched controls to about 0.3-fold of control. **Figure 5B** shows the results of a Western analysis of total NF-L protein (MW  $\sim 68 \text{ kDa}$ ) in control and AD neocortex (left panel) and control and LPS-treated HNG cells (right panel) using  $\beta$ -actin (MW  $\sim 42 \text{ kDa}$ ) as an internal control and gel-loading marker. **Figure 5C** shows the quantified results in bar graph format comparing NF-L protein abundance in AD and in age- and gender-matched control and in control and LPS-treated HNG cells. Therefore, the independent techniques of ELISA and Western analysis corroborated the observation that the normally highly abundant NF-L protein is reduced in both LPS-enriched AD-affected brain *in vivo* and in LPS-treated HNG cells *in vitro*. For additional experimental details please refer to the legend of **Figure 5**.

## DISCUSSION

### Gastrointestinal (GI) Tract Microbiome-Derived Neurotoxins in Neurological Disease

The human GI tract, containing about 95% of the entire human microbiome, is the largest reservoir of microorganisms in the human body (Bhattacharjee and Lukiw, 2013; Zhao and Lukiw, 2015; Zhan et al., 2016; Vogt et al., 2017; Zhao et al., 2017a; Zhao and Lukiw, 2018). Comprised of a genetically diverse and densely packed repository of about 100 trillion microorganisms, the GI-tract microbiome is made up of mostly of anaerobic bacterial species with archaeobacteria, fungi, protozoa, viruses, and other microbes making up the remainder (Bhattacharjee and Lukiw, 2013; Köhler et al., 2016; Vogt et al., 2017; Zhao et al., 2017a,b,c; Zhao and Lukiw, 2018). Microbial abundance, complexity and speciation, their biophysics, microbiology and neurobiology, molecular genetics, epigenetics, the signaling mechanisms, and pathways involved in microbiome-host communications and interactions are becoming increasingly understood in context of their dynamic contribution to human neurobiology in health, aging, and disease (Bhattacharjee and Lukiw, 2013; Foster et al., 2016; Köhler et al., 2016; Jiang et al., 2017; Cox and Weiner, 2018).

GI-tract derived neurotoxins include an extraordinarily complex mixture of potentially pathogenic amyloid, exotoxins and endotoxins, lipooligosaccharides (LOS), LPS, and small miRNA-like non-coding RNA (sncRNA) exudates. Normally confined within the healthy human GI-tract, accompanying aging, and disease these secreted neurotoxins can transverse normally protective biophysical and physiological barriers resulting in a persistent systemic inflammatory condition

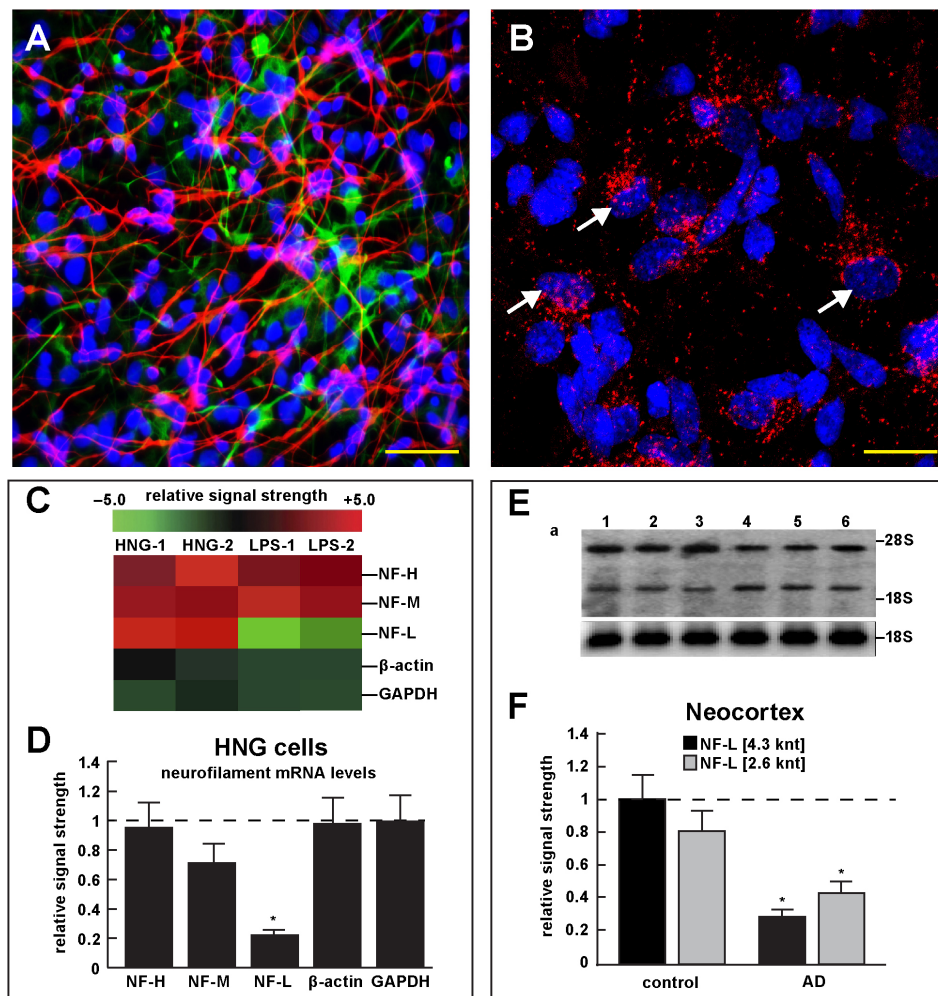


**FIGURE 4 |** Studies of LPS-neuronal nuclear binding in HNG cells in primary culture. **(A)** human neuronal-glial (HNG) cells in primary co-culture at 2 weeks; neurons (red stain;  $\lambda_{\max}$  = 690 nm), DAPI (blue nuclear stain;  $\lambda_{\max}$  = 470 nm) and GFAP (glial-specific green stain;  $\lambda_{\max}$  = 520 nm); human neurons do not culture well in the absence of glia; neurons also show both extensive arborization and display electrical activity (unpublished; Lonza); scale bar = 20  $\mu$ m; **(B)** details of association of LPS (red stain;  $\lambda_{\max}$  = 690 nm) and nuclear DAPI (blue stain;  $\lambda_{\max}$  = 470 nm); note affinity of red-stained LPS with blue-stained nuclei after only 48 h of co-incubation (arrows); see also **Supplementary File 1** (Details of accumulation of LPS in HNG cells in primary culture); scale bar for all photos (lower right) = 10  $\mu$ m; **(C)** Neurofilament heavy, medium and light (NF-H, NF-M, and NF-L) chain abundance in control and LPS-treated HNG cells – cluster analysis of gene expression (mRNA levels); in two controls (HNG-1 and HNG-2) and in two LPS-treated samples (LPS-1, LPS-2), LPS-treated HNG cells exhibit a marked reduction in NF-L expression, a reduction that is not as apparent in NF-H or NF-M expression; NF-H, NF-M, and NF-L expression was quantified against the levels of  $\beta$ -actin and GAPDH in the same sample; **(D)** samples are quantified in bar graph format showing the mean and one standard deviation of all three neurofilament protein levels; there was no statistically significant change in NF-H, NF-M,  $\beta$ -actin, or GAPDH between control and LPS-treated HNG cells, however NF-L levels were reduced to about 0.22-fold of controls in LPS-treated HNG cells; interestingly the NF-H, NF-M, and NF-L mRNAs encode intermediate filaments of ~60, ~100, and ~110 kDa, respectively, but due to extensive post-translational modifications such as phosphorylation and glycosylation, NF-H, NF-M, and NF-L exhibit higher molecular weights after SDS-PAGE (Western) analysis of ~68, ~160, and ~205 kDa, respectively; a dashed horizontal line at 1.0 is included for ease of comparison;  $N$  = 3 to 5 experiments for each treatment; \* $p$  < 0.01 (ANOVA); **(E)** Northern blot analysis – decreased NF-L in AD – Northern analysis of total NF-L mRNA in control (lanes 1–3) and AD (lanes 4–6) temporal lobe neocortex (Brodmann A22); the position of the migration of 28S and 18S RNA (4.7 and 1.9 knt, respectively) are marked on the right of the gel (upper panel); the size of the two prominent NF-L mRNA bands detected are respectively about 4.3 and 2.6 knt in length; an 18S RNA was used as an internal control marker (lower panel); **(F)** Northern blots were quantified in bar graph format showing the mean and one standard deviation of decreased NF-L mRNA signals in AD neocortex versus age-matched controls; in AD the 2 NF-L bands [between the 28S and 18S RNA markers of part **(E)**] together are about 0.3- to 0.4-fold AD over control; \* $p$  < 0.01 (ANOVA).

(Jiang et al., 2017; Magalhães et al., 2017). Leakage of GI-tract neurotoxins into the systemic circulation may be a biomarker and an early indicator of progressive, age-related neuroinflammatory disorders that include AD (Lukiw, 2017; Magalhães et al., 2017; Montagne et al., 2017; Cox and Weiner, 2018; Ho et al., 2018;

Sweeney et al., 2018). Indeed progressive “leakage” of LPS across the GI-tract and blood brain barrier (BBB) may be a feature accompanying normal aging (Montagne et al., 2017; Sweeney et al., 2018). Certain GI-tract microbiota may actively assist the host in moderating inflammatory neurodegeneration

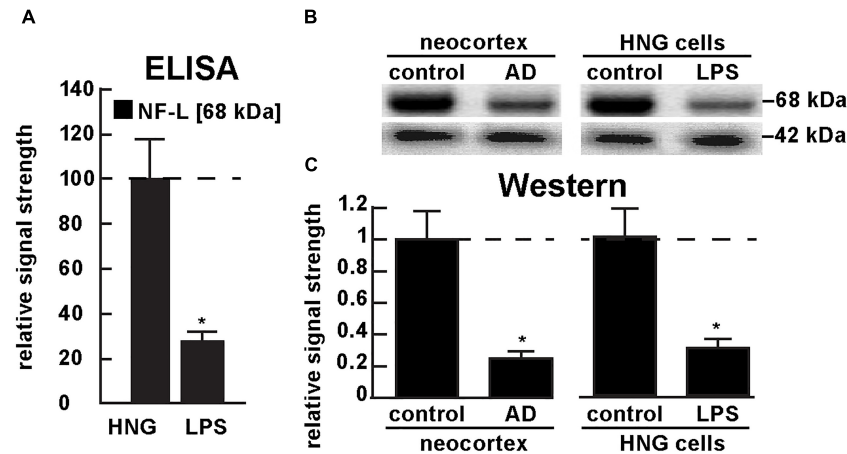


**FIGURE 5 |** Decreased NF-L protein in LPS-treated HNG cells and in AD: ELISA and Western analysis. **(A)** results of sandwich ELISA analysis for NF-L protein in LPS-treated HNG cells using Abxess (abx250460; Cambridge, United Kingdom) and/or LifeSpan BioSciences (LSBio; LS-F6701; Seattle WA, United States); the 68 kDa NF-L species is a particularly abundant intermediate filament protein, however in the presence of LPS the abundance of NF-L protein was found to be reduced to about 0.3-fold of control; a dashed horizontal line at 100 is included for ease of comparison;  $N = 3$  to 5 experiments per determination;  $*p < 0.01$  (ANOVA); **(B)** Western analysis of total NF-L protein (MW ~68 kDa) in control (pool of five controls and five AD temporal lobe neocortex Brodmann A22) and total NF-L protein in control and LPS-treated HNG cells (at 2 weeks of culture; see **Figure 4A**);  $\beta$ -actin protein (MW ~42 kDa) was used as an internal control marker in the same sample for each determination; **(C)** Western blots were quantified in bar graph format of decreased NF-L protein abundance in AD neocortex versus age-matched controls and in LPS-treated HNG cells versus age-matched controls; a dashed horizontal line at 1.0 is included for ease of comparison; the results of decreased NF-L expression for AD over control or LPS-treated HNG cells over control are highly significant;  $N = 3$  to 5 experiments;  $*p < 0.01$  (ANOVA).

by supporting the generation of short chain fatty acids (SCFAs) that can pass these barriers and subsequently interfere with the generation and aggregation of neurotoxic amyloid beta ( $A\beta$ ) peptides (Cox and Weiner, 2018; Ho et al., 2018). The interactions between LPS and amyloid peptides in the brain parenchyma remain incompletely understood, especially their dynamics and potential association as they accumulate in parallel with aging both within the confines of the CNS and throughout the systemic circulation (Zhao et al., 2017a,b,c).

## LPS Transit Across Biophysical and Physiological Barriers Into the CNS

Recent data regarding the contribution of neurotoxic exudates of the human GI tract microbiome to the potential initiation, development, and/or progression of AD appears to be age-related, complicated, and significant. Major bacterial species of the human GI-tract microbiome such as the Gram-negative bacillus *Bacteroides fragilis* (*B. fragilis*) secrete a unusually complex array of highly pathogenic pro-inflammatory neurotoxins which, when released from the confines of a healthy GI tract, are highly toxic to neurons of the CNS and PNS. While an environmental cause for sporadic AD has often been suggested, a strong source of powerful neurotoxins already reside within our GI tract microbiome. LPS for example represents an internally generated GI tract microbiome-derived neurotoxin capable of driving AD-type change and has enormous potential to initiate and/or propagate inflammatory neurodegeneration along the gut-brain axis. Some incompletely understood aspects of the bioavailability to the CNS of GI-tract generated neurotoxins are (i) their translocation through the GI tract and BBB that

involves dynamic structures which are known to become more “leaky” with aging and disease; (ii) the direct influence of endotoxins, such as fragilysin, which targets zonula adherens protein E-cadherin and cell–cell adhesion; and (iii) the molecular exchanges between the GI tract, the systemic circulation and the BBB to access the brain parenchyma (Seong et al., 2015; Zhan et al., 2016; Montagne et al., 2017; Tsou et al., 2017; Sweeney et al., 2018). To cite recent examples from the literature: (i) BF-LPS represents an internally generated GI tract microbiome-derived neurotoxin capable of driving and emulating AD-type change *in vitro* (Zhao and Lukiw, 2018); (ii) BF-LPS has enormous potential to initiate and/or propagate inflammatory neurodegeneration along the GI tract-CNS axis (Zhao et al., 2017a); and (iii) LPS has an unusually high and remarkable affinity for the periphery of neuronal nuclei of the human neocortex (**Figures 1–4**) (Zhao et al., 2017b).

## LPS and Perinuclear Association in Sporadic AD Brain

In middle-to-late-stage AD brain the perinuclear association of LPS in AD appears to be configured into “net-like” or “clathrin-like” lattice within the neuronal cell cytoplasm (**Figures 1–4**). The pyramidal neuronal nuclei of the human neocortex are among the largest known nuclei in the human CNS, often achieving diameters of 10–20  $\mu\text{m}$  and occupy a large proportion of the neuronal soma, conducive to their “euchromatic” nature and extremely high rates of transcription (Colangelo et al., 2002; Clement et al., 2016). The current experimental evidence further suggests that neuronal nuclear “encasement” by LPS appears to have a deleterious effect on the free exit and/or expression

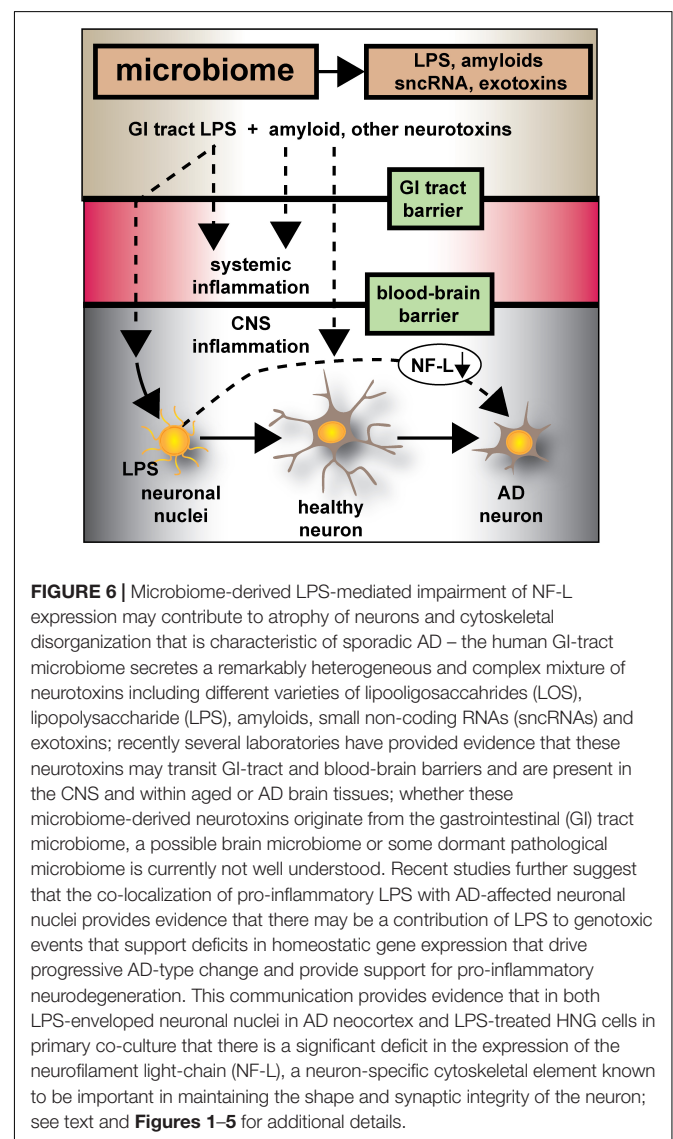
of mRNAs through the nuclear pores into the cytoplasm – previous work has shown a decreased rate of abundance of neuronal-specific DNA transcripts in sporadic AD brain (Zhao et al., 2017b). Why the NF-L mRNA exhibits the greatest down-regulated of the neurofilament triad is not known; the NF-L light chain polypeptide is the most abundant member of the neuron-specific intermediate filament family triplet, is the major component of the highly dynamic and plastic neurites, synaptic structures, and constitutes the core of the neuronal cytoskeleton. NF-L expression is also the major regulator of the caliber of the neuronal axoskeleton and essential in neuronal development, regeneration, the plasticity of the neuronal cytoskeleton, and in the creation and the maintenance of neuronal cytoarchitecture (Julien and Mushynski, 1998; Braissant, 2007; Lam et al., 2017; Goldmann, 2018; Abu-Rumeileh et al., 2018). NF-L also serves in a critical “organizer” role in axons and dendrites and contains multiple phosphorylation sites for a surprisingly large number of neuronal-enriched protein kinases, including protein kinase A, protein kinase C, cyclin-dependent kinase 5, extracellular signal regulated kinase, glycogen synthase kinase-3, and stress-activated protein kinase gamma (de Leeuw et al., 2018; Goldmann, 2018). Perturbations in NF-L phosphorylation, structure and/or function are often observed in age-related human neurodegenerative diseases including amyotrophic lateral sclerosis, Parkinson’s disease and AD, and a down-regulation of NF-L mRNA and the presence of atypical insoluble twisted neurofilament deposits have long been known to be a common feature of an abnormal neurofilament network as seen in diseased brain tissues undergoing pro-inflammatory neurodegeneration (McLachlan et al., 1988; Lukiw et al., 1990; Julien and Mushynski, 1998; Abu-Rumeileh et al., 2018; Goldmann, 2018; Zhao and Lukiw, 2018). Importantly, neuron loss in AD appears not to be the reason for the observed loss in NF-L; a classic study of 22 control, non-AD dementia and AD brains indicated that the significant decrease of NF-L mRNA in AD neocortex could not be adequately accounted for by a non-specific effect of brain damage, by neuron cell loss or by neurons with neurofibrillary degeneration (McLachlan et al., 1988; Julien and Mushynski, 1998; Ginsberg et al., 2000; Zhao et al., 2017a,b).

Interestingly, there are reports that plasma levels of NF-L protein appear to be increased in AD and may be used as a reliable diagnostic marker for AD incidence and severity (Lista et al., 2017; Abu-Rumeileh et al., 2018; Hampel et al., 2018). However, the universality of this elevation and usefulness of plasma NF-L as a biomarker for AD has been recently brought into question (Lam et al., 2017; Zhou et al., 2017; Abu-Rumeileh et al., 2018). Very recently NF-L has been found to be significantly increased in the CSF of early-onset AD patients compared to younger controls; however, this change was not found in older AD groups (Lauridsen et al., 2017). These discrepancies and differential localization of neuronal- and AD-relevant molecules are reminiscent of the variation in abundance of A $\beta$ 42 peptides within AD tissues and the extracellular fluids such as the CSF that surrounds them; for example A $\beta$ 42 peptides show an inverse abundance between brain tissues and the CSF (Fagan et al., 2006; Grimmer et al., 2009). Another example is potentially pathogenic microRNAs including a pro-inflammatory

miRNA-146a and several let-7 species which are differentially abundant in AD tissues versus the AD CSF (Alexandrov et al., 2012; Derkow et al., 2018). It is tempting to speculate that a differential “compartmentalization” of neuronal-associated AD-relevant molecular species may be one significant consequence of the neuropathology of the AD process.

## Important Unanswered Questions

Several fundamental questions remain concerning GI-tract microbiome exudates, their compartmentalization in the GI-tract and their potential effects on the neurobiology, neuropathology, and pathogenetics of neurodegenerative and neuropsychiatric disease. For example: does the presence of LPS and envelopment of neuronal nuclei in AD significantly affect the transcription of any other brain genes or neuron-enriched transcripts besides NF-L? Why are NF-L mRNA abundances selectively affected? Perhaps because NF-L expression is from an extremely high



output gene? Are the translocation of transcripts exiting the neuronal nuclei impaired by the envelopment of nuclei by LPS as they appear to be? Does a life-long exposure to certain infectious agents and their secreted neurotoxins predispose an individual to develop AD at a later age? How do the secreted neurotoxins from the human GI-tract microbiome progressively leak across biophysical and physiological barriers to access the systemic circulation and CNS compartments? Do these secreted neurotoxins interact with amyloid-beta ( $A\beta$ ) peptides that increase in parallel in the aging brain? What GI-tract bacterial-derived mixtures of neurotoxins are the most pathogenic in promoting inflammatory neuro-degeneration? Can the incidence of systemic inflammation be used as a biomarker or be of prognostic value to AD and other progressive neurodegenerative diseases? Does anaerobic Gram-negative bacilli-derived LPS interact pathologically with other toxins originating from archaeobacteria, fungi, protozoa, viruses, and other GI-tract resident microbes? Is there a potential synergism in their combined neurotoxic actions toward neuronal nuclei of the human CNS? Perhaps most importantly, is it possible to devise a dietary strategy that promotes the lowering of LPS secretion and optimize life-long GI-tract microbiome and CNS health to minimize the risk of developing AD as we age? Furthering our molecular and mechanistic understanding of how individual secreted components of the GI tract microbiome – affect the PNS and CNS may uncover potential and novel strategies for GI tract-based modulation of neural function and the more efficacious clinical management of terminal, age-related neurological disease.

## CONCLUSION

Microbiologists, neurologists and bioinformatics researchers are still in a relatively early stage of understanding the molecular-genetic pathological signaling mechanisms that operate between the human GI-tract microbiome and the CNS of the host. Emerging evidence suggests: (i) that non-homeostatic communication along the gut-brain axis may contribute to progressive inflammatory neurodegeneration and AD-type change in the CNS; and (ii) that the GI-tract microbiome appears to have potential to contribute to neurodegenerative disease through the release, and export into the systemic circulation, of multiple, highly pro-inflammatory neurotoxic exudates predominantly from abundant species of Gram-negative anaerobic bacteria such as *Bacteroides fragilis* and other GI-tract microbes (Bhattacharjee and Lukiw, 2013; Foster et al., 2016; Zhao et al., 2017b,c; Cox and Weiner, 2018; Zhan et al., 2018; Zhao and Lukiw, 2018). The co-localization and eventual envelopment of sporadic AD-affected neuronal nuclei with a “clathrin-like” cage of GI-tract microbiome-derived LPS suggests that there exists a novel pathogenic contribution of LPS to neuron-specific gene expression and transcriptional output from AD-affected neurons (Zhao et al., 2017b). In agreement with previous reports a remarkably high proportion of the LPS signal in AD neocortex and hippocampus and in LPS-treated HNG cells are associated with neuronal nuclei (Figures 1–5 and

**Supplementary File 1**; Zhao et al., 2017a,b,c; Zhao and Lukiw, 2018). Recent data further indicates that patients with moderate-to-advanced sporadic AD appear to have a significantly higher population of LPS-enveloped nuclei, and a correspondingly lower amount of NF-L associated with that region of the AD brain (Zhao et al., 2017b; Zhao and Lukiw, 2018) (Figures 5, 6).

In conclusion, the current work provides five novel observations: (i) that in AD neocortex LPS has a remarkable biophysical affinity for neuronal nuclei; (ii) that this action appears to selectively impair the transcriptional abundance of neuron-specific elements such as NF-L, known to be normally required for the maintenance of neuronal cytoarchitecture, synaptic connections, and the homeostatic signaling operations of neurons; (iii) that GI tract microbiome-derived neurotoxins may contribute to AD-type pathological and neuronal architectural change; (iv) that LPS-treated HNG brain cells in primary culture can recapitulate this phenomenon both at the biophysical and transcriptional level; and (v) perhaps most significantly, that LPS-treated HNG cells in primary culture can provide a highly useful experimental platform for further study on LPS effects on AD-like processes and their pathogenic consequences. These results also support the hypothesis that GI-tract derived, microbial neurotoxins such as LPS affect the efficient readout of AD-relevant neuronal-specific genetic information, such as that from the NF-L gene, and progressively contribute to cytoarchitectural aberrations, neuronal atrophy, and synaptic disorganization all of which are characteristic features of the sporadic AD brain (Figure 6).

## ETHICS STATEMENT

Procedures involving short post-mortem interval (PMI) human tissues and human brain primary cell cultures (HNG) were followed and handled in strict accordance with the ethics review board policies at donor institutions, and the Institutional Biosafety Committee/Institutional Review Board (IBC/IRB) ethical guidelines at the LSU Health Sciences Center, LA 70112, United States (IBC No. 12323; IRB No. 6774).

## AUTHOR CONTRIBUTIONS

LC, VJ, WL, and YZ preformed the experiments and analyzed the data. WL wrote the paper.

## FUNDING

Research on microRNAs, pro-inflammatory, and pathogenic signaling in the Lukiw Laboratory involving the microbiome, the innate-immune response, amyloidogenesis, synaptogenesis, and neuroinflammation in AD, prion, and in other neurological diseases was supported through an unrestricted grant to the LSU Eye Center from Research to Prevent Blindness (RPB); the Louisiana Biotechnology Research Network (LBRN), and NIH grants NEI EY006311, NIA AG18031, and NIA AG038834 (WL).

## ACKNOWLEDGMENTS

The experimental work in this paper was presented in part at the Vavilov Institute of General Genetics/Moscow State University Autumn 2017 Seminar Series (Институт общей генетики имени Вавилова Осень 2017 Семинар серии) in Moscow, RUSSIA October 2017 and at the Society for Neuroscience (SFN) Annual Meeting, Washington, DC, United States November 2017. We would like to express our sincere thanks to Drs L. Carver, L. Cong, J. G. Cui, F. Culicchia, C. Eicken, V. Jaber, K. Navel, A. I. Pogue, W. Poon and the late Drs. J. M. Hill and T. P. Kruck for helpful discussions in this research area, for short post-mortem interval (PMI) human brain, and HNG cells or extracts, for initial bioinformatics and data interpretation, and to D Guillot for expert technical assistance and medical artwork. Thanks are also extended to the University of California at Irvine Brain Bank, the University of

Maryland Brain Bank, the Harvard Brain Tissue Resource Center, the LSU School of Medicine, and the many neuropathologists, physicians, and researchers in the United States and Canada who have provided high quality, short PMI human brain tissue fractions for scientific analysis. The content of this manuscript is solely the responsibility of the authors and does not necessarily represent the official views of the National Institute on Aging, the National Center for Research Resources, or the National Institutes of Health.

## SUPPLEMENTARY MATERIAL

The Supplementary Material for this article can be found online at: <https://www.frontiersin.org/articles/10.3389/fnins.2018.00896/full#supplementary-material>

## REFERENCES

- Abu-Rumeileh, S., Capellari, S., Stanzani-Maserati, M., Polisch, B., Martinelli, P., Caroppo, P., et al. (2018). The CSF neurofilament light signature in rapidly progressive neurodegenerative dementias. *Alzheimers Res. Ther.* 10:3. doi: 10.1186/s13195-017-0331-1
- Alexandrov, P. N., Dua, P., Hill, J. M., Bhattacharjee, S., Zhao, Y., and Lukiw, W. J. (2012). microRNA (miRNA) speciation in Alzheimer's disease (AD) cerebrospinal fluid (CSF) and extracellular fluid (ECF). *Int. J. Biochem. Mol. Biol.* 3, 365–373.
- Bagyinszky, E., Giau, V. V., Shim, K., Suk, K., An, S. S. A., and Kim, S. (2017). Role of inflammatory molecules in the Alzheimer's disease progression and diagnosis. *J. Neurol. Sci.* 376, 242–254. doi: 10.1016/j.jns.2017.03.031
- Bhattacharjee, S., and Lukiw, W. J. (2013). Alzheimer's disease and the microbiome. *Front. Cell Neurosci.* 7:153. doi: 10.3389/fncel.2013.00153
- Braissant, O. (2007). "Neurofilament proteins in brain diseases," in *New Research on Neurofilament Proteins* ISBN: 1-60021-396-0, ed. R. K. Arlen (Hauppauge, NY: Nova Science Publishers, Inc), 25–51.
- Clark, I. A., and Vissel, B. (2015). Amyloid  $\beta$ : one of three danger-associated molecules that are secondary inducers of the proinflammatory cytokines that mediate AD. *Br. J. Pharmacol.* 172, 3714–3727. doi: 10.1111/bph.13181
- Clement, C., Hill, J. M., Dua, P., Culicchia, F., and Lukiw, W. J. (2016). Analysis of RNA from Alzheimer's disease post-mortem brain tissues. *Mol. Neurobiol.* 53, 1322–1328. doi: 10.1007/s12035-015-9105-6
- Colangelo, V., Schurr, J., Ball, M. J., Pelaez, R. P., Bazan, N. G., and Lukiw, W. J. (2002). Gene expression profiling of 12633 genes in Alzheimer hippocampal CA1: transcription and neurotrophic factor down-regulation and up-regulation of apoptotic and pro-inflammatory signaling. *J. Neurosci. Res.* 70, 462–473. doi: 10.1002/jnr.10351
- Cox, L. M., and Weiner, H. L. (2018). Microbiota signaling pathways that influence neurologic disease. *Neurotherapeutics* 15, 135–145. doi: 10.1007/s13311-017-0598-8
- Cui, J. G., Li, Y. Y., Zhao, Y., Bhattacharjee, S., and Lukiw, W. J. (2010). Differential regulation of interleukin-1 receptor-associated kinase-1 (IRAK-1) and IRAK-2 by microRNA-146a and NF- $\kappa$ B in stressed human astroglial cells and in Alzheimer disease. *J. Biol. Chem.* 285, 38951–38960. doi: 10.1074/jbc.m110.178848
- de Leeuw, R., Gruenbaum, Y., and Medalia, O. (2018). Nuclear lamins: thin filaments with major functions. *Trends Cell Biol.* 28, 34–45. doi: 10.1016/j.tcb.2017.08.004
- Dendooven, T., and Luisi, B. F. (2017). RNA search engines empower the bacterial intranet. *Biochem. Soc. Trans.* 45, 987–997. doi: 10.1042/BST20160373
- Derkow, K., Rössling, R., Schipke, C., Krüger, C., Bauer, J., Fähring, M., et al. (2018). Distinct expression of the neurotoxic microRNA family let-7 in the cerebrospinal fluid of patients with Alzheimer's disease. *PLoS One* 13:e0200602. doi: 10.1371/journal.pone.0200602
- Fagan, A. M., Mintun, M. A., Mach, R. H., Lee, S. Y., Dence, C. S., Shah, A. R., et al. (2006). Inverse relation between in vivo amyloid imaging load and cerebrospinal fluid A $\beta$ 42 in humans. *Ann. Neurol.* 59, 512–519. doi: 10.1002/ana.20730
- Foster, J. A., Lyte, M., Meyer, E., and Cryan, J. F. (2016). Gut microbiota and brain function: an evolving field in neuroscience. *Int. J. Neuropsychopharmacol.* 19:yy114. doi: 10.1093/ijnp/pyv114
- Ginsberg, S. D., Hemby, S. E., Lee, V. M., Eberwine, J. H., and Trojanowski, J. Q. (2000). Expression profile of transcripts in Alzheimer's disease tangle-bearing CA1 neurons. *Ann. Neurol.* 48, 77–87. doi: 10.1002/1531-8249(200007)48:1<77::AID-ANA12>3.0.CO;2-A
- Goldmann, W. H. (2018). Intermediate filaments and cellular mechanics. *Cell Biol. Int.* 42, 132–138. doi: 10.1002/cbin.10879
- Grimmer, T., Riemenschneider, M., Förstl, H., Henriksen, G., Klunk, W. E., Mathis, C. A., et al. (2009). Beta amyloid in Alzheimer's disease: increased deposition in brain is reflected in reduced concentration in cerebrospinal fluid. *Biol. Psychiatry* 65, 927–934. doi: 10.1016/j.biopsych.2009.01.027
- Hampel, H., Toschi, N., Baldacci, F., Zetterberg, H., Blennow, K., Kilimann, I., et al. (2018). Alzheimer's disease biomarker-guided diagnostic workflow using the added value of six combined cerebrospinal fluid candidates: A $\beta$ (1-42), total-tau, phosphorylated-tau, NFL, neurogranin, and YKL-40. *Alzheimers Dement.* 14, 492–501. doi: 10.1016/j.jalz.2017.11.015
- Ho, L., Ono, K., Tsuji, M., Mazzola, P., Singh, R., Pasinetti, G. M. et al. (2018). Protective roles of intestinal microbiota derived short chain fatty acids in Alzheimer's disease-type beta-amyloid neuropathological mechanisms. *Expert Rev. Neurother.* 18, 83–90. doi: 10.1080/14737175.2018.1400909
- Hofer, U. (2014). Microbiome: *B. fragilis* and the brain. *Nat. Rev. Microbiol.* 12, 76–77. doi: 10.1038/nrmicro3197
- Jaber, V., Zhao, Y., and Lukiw, W. J. (2017). Alterations in micro RNA-messenger RNA (miRNA-mRNA) coupled signaling networks in sporadic Alzheimer's disease (AD) hippocampal CA1. *J. Alzheimers Dis. Parkinsonism* 7:312. doi: 10.4172/2161-0460.1000312
- Jiang, C., Li, G., Huang, P., Liu, Z., and Zhao, B. (2017). The gut microbiota and Alzheimer's disease. *J. Alzheimers Dis.* 58, 1–15. doi: 10.3233/JAD-161141
- Julien, J. P., and Mushynski, W. E. (1998). Neurofilaments in health and disease. *Prog. Nucleic Acid Res. Mol. Biol.* 61, 1–23. doi: 10.1016/S0079-6603(08)60823-5
- Khalil, B., Morderer, D., Price, P. L., Liu, F., and Rossoll, W. (2018). mRNP assembly, axonal transport, and local translation in neurodegenerative diseases. *Brain Res.* 1693(Pt A), 75–91. doi: 10.1016/j.brainres.2018.02.018
- Köhler, C. A., Maes, M., Slyepchenko, A., Berk, M., Solmi, M., Lanctôt, K. L., et al. (2016). The gut-brain axis, including the microbiome, leaky gut and bacterial translocation: mechanisms and pathophysiological role in Alzheimer's disease. *Curr. Pharm. Des.* 22, 6152–6166. doi: 10.2174/1381612822666160907093807
- Lam, K. Y. C., Huang, Y., Yao, P., Wang, H., Dong, T. T. X., Zhou, Z., et al. (2017). Comparative study of different acorus species in potentiating neuronal

- differentiation in cultured PC12 cells. *Phytother. Res.* 31, 1757–1764. doi: 10.1002/ptr.5904
- Lauridsen, C., Sando, S. B., Möller, I., Berge, G., Pomary, P. K., Grøntvedt, G. R., et al. (2017). Cerebrospinal fluid Aβ43 is reduced in early-onset compared to late-onset Alzheimer's disease, but has similar diagnostic accuracy to Aβ42. *Front. Aging Neurosci.* 9:210. doi: 10.3389/fnagi.2017.00210
- Li, Y. Y., Cui, J. G., Dua, P., Pogue, A. I., Bhattacharjee, S., and Lukiw, W. J. (2011). Differential expression of miRNA-146a-regulated inflammatory genes in human primary neural, astroglial and microglial cells. *Neurosci. Lett.* 499, 109–113. doi: 10.1016/j.neulet.2011.05.044
- Lista, S., Toschi, N., Baldacci, F., Zetterberg, H., Blennow, K., Kilimann, I., et al. (2017). Diagnostic accuracy of CSF neurofilament light chain protein in the biomarker-guided classification system for Alzheimer's disease. *Neurochem. Int.* 108, 355–360. doi: 10.1016/j.neuint.2017.05.010
- Lukiw, W. J. (2016a). *Bacteroides fragilis* lipopolysaccharide and inflammatory signaling in Alzheimer's disease. *Front. Microbiol.* 7:1544. doi: 10.3389/fmicb.2016.01544
- Lukiw, W. J. (2016b). The microbiome, microbial-generated pro-inflammatory neurotoxins, and Alzheimer's disease. *J. Sport Health Sci.* 5, 393–396. doi: 10.1016/j.jshs.2016.08.008
- Lukiw, W. J. (2017). The microbiome, microbial-generated pro-inflammatory neurotoxins, and Alzheimer's disease. *J. Sport Health Sci.* 5, 393–396. doi: 10.1016/j.jshs.2016.08.008
- Lukiw, W. J., Cui, J. G., Marcheselli, V. L., Bodker, M., Botkjaer, A., Gotlinger, K., et al. (2005). A role for docosahexaenoic acid-derived neuroprotectin D1 in neural cell survival and Alzheimer disease. *J. Clin. Invest.* 115, 2774–2783. doi: 10.1172/JCI25420
- Lukiw, W. J., Wong, L., and McLachlan, D. R. C. (1990). Cytoskeletal messenger RNA stability in human neocortex: studies in normal aging and in Alzheimer's disease. *Int. J. Neurosci.* 55, 81–88. doi: 10.3109/00207459008985953
- Magalhães, T. N. C., Weiler, M., Teixeira, C. V. L., Hayata, T., Moraes, A. S., Boldrini, V. O., et al. (2017). Systemic inflammation and multimodal biomarkers in amnesic mild cognitive impairment and Alzheimer's disease. *Mol. Neurobiol.* 55, 5689–5697. doi: 10.1007/s12035-017-0795-9
- Mancuso, C., and Santangelo, R. (2017). AD and gut microbiota modifications: the long way between preclinical studies and clinical evidence. *Pharmacol. Res.* 129, 329–336. doi: 10.1016/j.phrs.2017.12.009
- McLachlan, D. R. C., Lukiw, W. J., Wong, L., Bergeron, C., and Bech-Hansen, N. T. (1988). Selective messenger RNA reduction in Alzheimer's disease. *Brain Res.* 427, 255–261. doi: 10.1016/0169-328X(88)90048-4
- Minter, M. R., Taylor, J. M., and Crack, P. J. (2016). The contribution of neuroinflammation to amyloid toxicity in Alzheimer's disease. *J. Neurochem.* 136, 457–474. doi: 10.1111/jnc.13411
- Montagne, A., Zhao, Z., and Zlokovic, B. V. (2017). Alzheimer's disease: a matter of blood-brain barrier dysfunction? *J. Exp. Med.* 214, 3151–3169. doi: 10.1084/jem.20171406
- Seong, E., Yuan, L., and Arikath, J. (2015). Cadherins and catenins in dendrite and synapse morphogenesis. *Cell Adh Migr.* 9, 202–213. doi: 10.4161/19336918.2014.994919
- Sweeney, M. D., Sagare, A. P., and Zlokovic, B. V. (2018). Blood-brain barrier breakdown in Alzheimer disease and other neurodegenerative disorders. *Nat. Rev. Neurol.* 14, 133–150. doi: 10.1038/nrneurol.2017.188
- Szablewski, L. (2018). Human gut microbiota in health and Alzheimer's disease. *J. Alzheimers Dis.* 62, 549–560. doi: 10.3233/JAD-170908
- Tsou, Y. H., Zhang, X. Q., Zhu, H., Syed, S., and Xu, X. (2017). Drug delivery to the brain across the blood-brain barrier using nanomaterials. *Small* 13:1701921. doi: 10.1002/smll.201701921
- Vogt, N. M., Kerby, R. L., Dill-McFarland, K. A., Harding, S. J., Merluzzi, A. P., Johnson, S. C., et al. (2017). Gut microbiome alterations in Alzheimer's disease. *Sci. Rep.* 7:13537. doi: 10.1038/s41598-017-13601-y
- Yang, N. J., and Chiu, I. M. (2017). Bacterial signaling to the nervous system through toxins and metabolites. *J. Mol. Biol.* 429, 587–605. doi: 10.1016/j.jmb.2016.12.023
- Zhan, X., Stamova, B., Jin, L. W., DeCarli, C., Phinney, B., and Sharp, F. R. (2016). Gram-negative bacterial molecules associate with Alzheimer disease pathology. *Neurology* 87, 2324–2332. doi: 10.1212/WNL.0000000000003391
- Zhan, X., Stamova, B., and Sharp, F. R. (2018). Lipopolysaccharide associates with amyloid plaques, neurons and oligodendrocytes in Alzheimer's disease brain. *Front. Aging Neurosci.* 10:42. doi: 10.3389/fnagi.2018.00042
- Zhao, Y., Bhattacharjee, S., Jones, B. M., Hill, J., Dua, P., and Lukiw, W. J. (2014). Regulation of neurotropic signaling by the inducible, NF-κB-sensitive miRNA-125b in Alzheimer's disease (AD) and in primary human neuronal-glia (HNG) cells. *Mol. Neurobiol.* 50, 97–106. doi: 10.1007/s12035-013-8595-3
- Zhao, Y., Calon, F., Julien, C., Winkler, J. W., Petasis, N. A., Lukiw, W. J., et al. (2011). Docosahexaenoic acid-derived neuroprotectin D1 induces neuronal survival via secretase- and PPARγ-mediated mechanisms in Alzheimer's disease models. *PLoS One* 6:e15816. doi: 10.1371/journal.pone.0015816
- Zhao, Y., Cong, L., Jaber, V., and Lukiw, W. J. (2017a). Microbiome-derived lipopolysaccharide enriched in the perinuclear region of Alzheimer's disease brain. *Front. Immunol.* 8:1064. doi: 10.3389/fimmu.2017.01064
- Zhao, Y., Cong, L., and Lukiw, W. J. (2017b). Lipopolysaccharide (LPS) accumulates in neocortical neurons of Alzheimer's disease (AD) brain and impairs transcription in human neuronal-glia primary co-cultures. *Front. Aging Neurosci.* 9:407. doi: 10.3389/fnagi.2017.00407
- Zhao, Y., Jaber, V., and Lukiw, W. J. (2017c). Secretory products of the human GI tract and their potential impact on Alzheimer's disease (AD): detection of lipopolysaccharide (LPS) in AD Hippocampus. *Front. Cell. Infect. Microbiol.* 7:318. doi: 10.3389/fcimb.2017.00318
- Zhao, Y., and Lukiw, W. J. (2015). Microbiome-generated amyloid and potential impact on amyloidogenesis in Alzheimer's disease (AD). *J. Nat. Sci.* 1:e138.
- Zhao, Y., and Lukiw, W. J. (2018). Microbiome-mediated upregulation of microRNA-146a in sporadic Alzheimer's disease. *Front. Neurol.* 9:145. doi: 10.3389/fneur.2018.00145
- Zhou, W., Zhang, J., Ye, F., Xu, G., Su, H., Su, Y., et al. (2017). Alzheimer's disease neuroimaging initiative. plasma neurofilament light chain levels in Alzheimer's disease. *Neurosci. Lett.* 650, 60–64. doi: 10.1016/j.neulet.2017.04.027

**Conflict of Interest Statement:** The authors declare that the research was conducted in the absence of any commercial or financial relationships that could be construed as a potential conflict of interest.

Copyright © 2018 Lukiw, Cong, Jaber and Zhao. This is an open-access article distributed under the terms of the Creative Commons Attribution License (CC BY). The use, distribution or reproduction in other forums is permitted, provided the original author(s) and the copyright owner(s) are credited and that the original publication in this journal is cited, in accordance with accepted academic practice. No use, distribution or reproduction is permitted which does not comply with these terms.